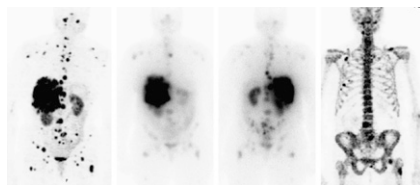


# THIS MONTH IN JNM

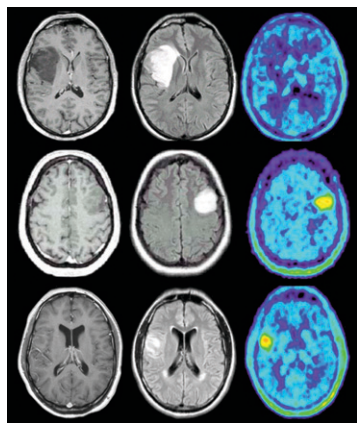
**Patient-friendly dose calculation:** Sgouros reviews the recent history of and challenges to clinical dosimetry in targeted radionuclide therapy and previews an article in this issue of *JNM* that offers a novel approach for cell-level dosimetry. . . . . **Page 496**

**Beyond SPECT in SSR imaging:** Schillaci outlines the current status of somatostatin receptor scintigraphy, CT, and PET imaging of neuroendocrine tumors and previews an article in this issue of *JNM* that describes a promising PET tracer. . . . . **Page 498**

**<sup>18</sup>F-FDG in MTC:** Ong and colleagues assess the effect of postthyroidectomy calcitonin levels on the ability of <sup>18</sup>F-FDG PET and PET/CT to detect residual, recurrent, or metastatic medullary thyroid carcinoma. . . . . **Page 501**

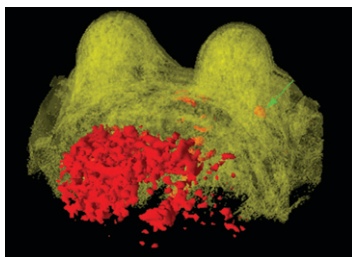


**Novel PET tracer for NETs:** Gabriel and colleagues evaluate the diagnostic efficacy of a new gadolinium-labeled somatostatin analog for PET imaging in patients with known or suspected neuroendocrine tumors and compare clinical results with those from scintigraphy and CT. . . . **Page 508**

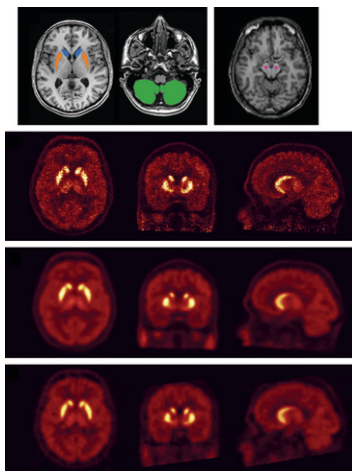


**PET and MRI in glioma management:** Floeth and colleagues identify <sup>18</sup>F-FET PET and MRI characteristics that are validated as strong predictors of clinical course and outcome in adult patients with newly diagnosed, nonenhancing, supratentorial low-grade glioma. . . . . **Page 519**

**Prone PET/MRI fusion in breast cancer:** Moy and colleagues describe a prototype positioning device that allows the acquisition of prone PET studies to facilitate fusion of <sup>18</sup>F-FDG PET and MRI scans for enhanced detection of breast cancer. . . . . **Page 528**

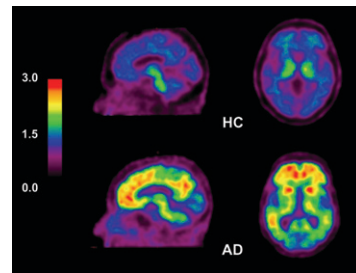


**Dedicated, high-resolution neuroimaging:** Leroy and colleagues evaluate the clinical utility of high-resolution research tomography for measurement of dopamine transporter binding and compare the spatial resolutions achieved with those of conventional PET scanners. . . . . **Page 538**



**Simplifying PET amyloid imaging:** Ng and colleagues explore the potential of

<sup>11</sup>C-PIB PET for the diagnosis of Alzheimer's disease and compare visual analysis of PIB images with visual readings of <sup>18</sup>F-FDG images. . . . . **Page 547**

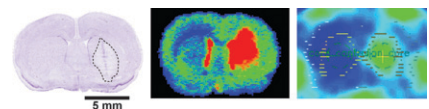


**Imaging dense amyloid plaques:** Kudo and colleagues report on a novel compound for in vivo PET detection of dense amyloid deposits and describe initial findings in healthy individuals and patients with Alzheimer's disease. . . . **Page 553**

**Detecting apoptosis in heart failure:** Kietse-laer and colleagues evaluate the utility of annexin A5 imaging for noninvasive assessment of programmed cell death in patients with advanced nonischemic cardiomyopathy and in nonsymptomatic genetic relatives. . . **Page 562**

**Standardized 4-hour gastric emptying:** Ziessman and colleagues review their experience with a standardized protocol for gastric-emptying studies and investigate the added value of 4-h imaging as well as the ability of the lag phase to predict delayed emptying. . . . . **Page 568**

**PET and neuronal stress:** Boutin and colleagues investigate a new peripheral benzodiazepine receptor ligand suitable for PET monitoring of neuroinflammatory processes as an indirect indicator of neurodegeneration. . . . . **Page 573**



**Antigen targeting and plaques:** von Lukowicz and colleagues test the ability of the human antibody G11, specific to the C domain of tenascin-C, to detect murine

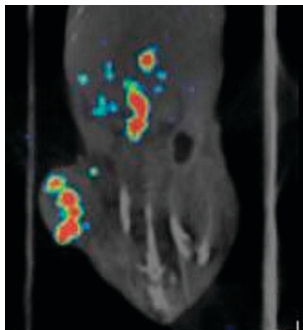
atherosclerotic plaques ex vivo and discuss the implications of their findings for molecular imaging. . . . . **Page 582**

**Dual membrane–protein reporter system:** Hwang and colleagues describe a combination of human sodium iodide symporter and mutant dopamine D<sub>2</sub> receptor transgenes to create a noninvasive positron and  $\gamma$ -imaging reporter system capable of noninvasive monitoring of cellular status. . . . **Page 588**

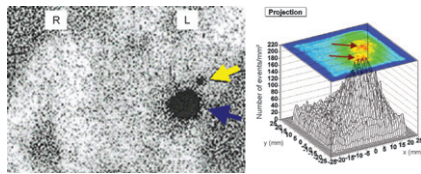
**Limiting PRRT nephrotoxicity:** Gotthardt and colleagues evaluate the ability of several agents to inhibit renal accumulation of different radiopeptides in an effort to enhance the efficacy of peptide receptor radiotherapy. . . . **Page 596**

**microPET study reliability:** Dandekar and colleagues determine the reproducibility of serial <sup>18</sup>F-FDG small-animal PET imaging in mouse xenograft models to assess the efficacy of this approach in measuring tumor response to therapy. . . . . **Page 602**

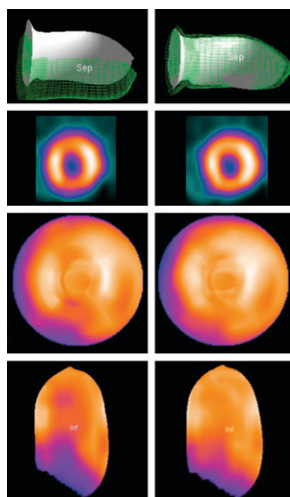
**Optimal angiogenesis monitoring:** Wyss and colleagues measure uptake of three <sup>18</sup>F-labeled PET tracers in gliomas in a rat model and correlate their findings with the uptake of a radiolabeled anti–extra domain B antibody as a marker of neoangiogenesis. . **Page 608**



**Radiolabeled gastrin analogs:** Mather and colleagues report on a study designed to identify a radiolabeled peptide with improved tumor-to-kidney pharmacodynamics for peptide receptor radionuclide imaging and therapy. . . . . **Page 615**



**Intraoperative  $\gamma$ -camera in breast cancer:** Mathelin and colleagues report on the ability of a prototype mini  $\gamma$ -camera to precisely localize and determine the depth of sentinel lymph nodes in a series of patients with infiltrative breast cancer. . . . . **Page 623**

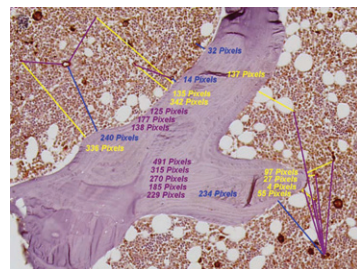


**Respiratory gating in SPECT:** Gil and colleagues describe a technique for correcting the respiration effect in myocardial

perfusion imaging and assess its efficacy in clinical studies. . . . . **Page 630**

**Correcting 3D <sup>201</sup>Tl SPECT:** Xiao and colleagues report on a Monte Carlo–based scatter correction approach that is suitable for <sup>201</sup>Tl cardiac imaging and also describe benefits noted in several image-quality metrics. . . . . **Page 637**

**Dosimetry and target cell distribution:** Watchman and colleagues describe direct measurement of hematopoietic and progenitor cells as well as marrow vasculature structures within images of human disease-free bone marrow. . . . . **Page 645**



**Assessing gene therapy:** Nimmagadda and colleagues investigate the biodistribution, metabolism, and DNA uptake of <sup>18</sup>F-FIAU in a canine model and report on the potential of this tracer as a reporter probe to monitor HSV-tk gene expression and bacterial infections. . . . . **Page 655**

**All about SPECT:** Madsen presents an educational overview of basic physics and recent innovations in SPECT imaging and instrumentation, including the advantages leveraged by new preclinical small-animal systems capable of providing information unavailable from other modalities. . . . . **Page 661**

## ON THE COVER

A novel PET compound has displayed preferential binding to dense amyloid deposits in the brains of patients with Alzheimer’s disease. The tracer is retained in the cerebral cortices of the patients but not of aged healthy individuals and is distributed primarily in the posterior association area of the brain, corresponding well with the preferred site for neuritic plaque deposition. This compound is a promising PET probe for the in vivo detection of dense amyloid deposits in Alzheimer’s disease patients.

SEE PAGE 560

